Solid-State Mechanical Properties of Polypropylene/Nylon 6/Clay Nanocomposites

A. Somwangthanaroj, W. Ubankhlong, W. Tanthapanichakoon

Department of Chemical Engineering, Faculty of Engineering, Chulalongkorn University, Bangkok 10330, Thailand

Received 15 January 2009; accepted 22 February 2010
DOI 10.1002/app.32328
Published online 21 May 2010 in Wiley InterScience (www.interscience.wiley.com).

ABSTRACT: The mechanical and thermomechanical properties as well as microstructures of polypropylene/nylon 6/clay nanocomposites prepared by varying the loading of PP-MA compatibilizer and organoclay (OMMT) were investigated. The compatibilizer PP-MA was used to improve the adhesion between the phases of polymers and the dispersion of OMMT in polymer matrix. Improvement of interfacial adhesion between the PP and PA6 phases occurred after the addition of PP-MA as confirmed by SEM micrographs. Moreover, as shown by the DSC thermograms and XRD results, the degree of crystallinity of PA6 decreased in the presence of PP-MA. The presence of OMMT increased the tensile modulus as a function of OMMT loading due to the good dispersion of OMMT in the matrix. The insertion of polymer chains between clay platelets was verified by both XRD and TEM techniques. The viscosity of the nanocomposites decreased as PP-MA loading increased due to the change in sizes of PA6 dispersed phase, and the viscosity increased as OMMT loading increased due to the interaction between the clay platelets and polymer chains. The clay platelets were located at the interface between PP and PA6 as confirmed by both SEM and TEM.
 J Appl Polym Sci 118: 538–546, 2010

Key words: nanocomposites; blends; organoclay; mechanical properties

INTRODUCTION

Blending two or more polymers together or a polymer with inorganic fillers to obtain a polymer blend or polymer composite, respectively, is an effective technique to improve the properties of these materials. However, many pairs of polymers are almost impossible to mix or disperse in one another, thereby yielding rather useless coarse aggregates with little or no adhesion between the phases. The minor component forms domains, whose size and shape greatly depend on several factors, such as melt viscosity of the component, interfacial tension, adhesiveness, and processing conditions. Polypropylene (PP) and nylon 6 (PA6) make a pair of polymers which have different polarities. This couple is not compatible if no compatibilizer is added to reduce interfacial tension between the phases. Added as a third component, an appropriate compatibilizer either induces an *in situ* chemical reaction or uses reactive blending to improve interfacial interaction and stress transfer. Polypropylene grafted maleic anhydride (PP-MA) was used as a reactive compatibilizer in the PP/PA6 blend because the blend with PP-MA showed greater enhancement in physical properties such as morphological,[1–3] mechanical,[2,4–6] and thermal properties[2,5] than that with other compatibilizers. Not only PP-MA but also polypropylene functionalized glycidyl methacrylate, (PP-GMA),[7] poly(oxypropylene)-amide grafted polypropylene (POP) with PP-MA,[8] maleic anhydride-*graft*-ethylene–propylene rubber (EPR-*g*-MA),[4] and maleated styrene–ethylene–butylene–styrene (SEBS-*g*-MA)[9] were also used as compatibilizers. The main reason for property improvement is good adhesion between the two phases, whereby the compatibilizer adhered between the different polymeric phases via a copolymerization process. Moreover, the compatibilizer was often used to reduce surface tension between a pair of polymers. Usually, the compatibilizer was added to the polymer nanocomposite to enhance the degree of dispersion of some nanofiller in the polymer matrix.

The development of new polymeric properties may use various techniques other than polymer blending such as adding some reinforcing filler into the polymer. The reinforcing filler might enhance mechanical properties, reduces compound cost, provides good resistance against moisture, chemicals and temperature, and ensures good processability. In addition, the composite is amenable to recycling with minimal sacrifice in physical properties.[10] Recently, nanocomposites, polymer composites filled with nanometer-sized particles, have been developed

Correspondence to: A. Somwangthanaroj (anongnat.s@chula.ac.th).

Contract grant sponsors: Thailand Research Fund (TRF), Commission on Higher Education (CHE), The Graduate School of Chulalongkorn University.

to overcome limitations of traditional micrometer-scale polymer composites. Nanofillers with at least one-dimension smaller than 100 nm possess unique properties by themselves. Nanocomposites were observed to exhibit higher Young's moduli than fiber-filled composites.[11] Because of their advantages, polymer nanocomposites have intensively been investigated both in industrial and academic fields. Investigations have been done not only on homopolymer nanocomposites such as polyethylene,[12,13] polypropylene,[14,15] polyurethane,[16] polystyrene[17] but also on polymer blend nanocomposites such as PC/ABS,[18] PEO/PMM,[19] and PA6/PP.[4,20]

In this study, nanocomposites of polymer blend between PP and PA6 were developed. Although Chow et al. used the morphology and FTIR results to propose the possible reaction between PP, PA6, and compatiblizer which affected the properties of nanocomposites, our work varied the loading of PP-MA compatibilizer and organoclay and investigated the effects of the compatibilizer and organoclay loadings on crystal structure, degree of crystallinity, degree of organoclay dispersion, and microstructure of nanocomposites which in turn affects the solid-state mechanical and thermomechanical properties as well as melt state processibility of nanocomposites. More specifically, PP/PA6/clay nanocomposites were prepared with a twin screw extruder and, subsequently, an injection molding machine. The degree of clay dispersion was evaluated by means of X-ray diffraction and TEM. The compatibility between the PP and PA6 phases was observed on SEM micrographs. In addition, the locations of the clay in the polymer blend were identified with SEM and TEM. The degree of crystallinity, crystal phases and thermomechanical behavior of the polymers, and their nanocomposites were characterized with DSC, XRD, and DMA, respectively. The mechanical properties of the blends and nanocomposites were investigated by means of tensile, flexural, and impact tests. Moreover, the rheological behavior of the nanocomposites was characterized with a rheometer in the linear viscoelastic regime.

EXPERIMENTAL

Materials

Polypropylene (PP, HP648N) was obtained from HMC, Thailand. Polyamide 6 or nylon 6 (PA6, 1015B) was obtained from UBE NYLON, Thailand. As compatibilizer, polypropylene-*graft*-maleic anhydride (PP-MA, MZ109D) was obtained from Innovation Group, Thailand. The melt flow index (MFI) of PP-MA is 120 g/min, according to ASTM D1238 at 0.55 wt % of maleic anhydride. Organophilic montmorillonite (OMMT, Bentone SD-2) was supplied by Connell Bros., Thailand and was used as received. According to product literature, the clay is organically modified montmorillonite (OMMT).

Blend preparation

The blend components were manually premixed before undergoing the melt mixing process. In this study, all polymer blends and polymer/clay nanocomposites (PP/PA6/PPMA/organoclay) were obtained by the melt mixing method. Because PP-MA, PA6, and organoclay could readily absorb moisture from the air, they were completely dried overnight in a vacuum oven at 80°C to eliminate the hydrolyzing effect of absorbed water. The screw rotation speed was set at 230 rpm and the temperature, 230°C. The sample code used in this study indicates the weight ratio of S : PP-MA : OMMT, in which S or the weight ratio of PP : PA 6 is kept constant at 13 : 6 by weight.

Characterization

To observe the size and shape of nylon 6 domains in PP matrix, the samples were immersed in liquid nitrogen and cryofractured. After that, nylon 6 domains were removed from the samples by immersing the samples in formic acid at room temperature for 24 h. The samples were then washed with fresh solvent, and dried at 40°C until constant weight was attained. The samples with smoothly fractured surfaces were then sputtered with gold and made ready for imaging. SEM micrographs were obtained with a Scanning Electron Microscope (JEOL, JSM-5400) at an acceleration voltage of 10 kV.

Tensile testing according to ASTM D638 was carried out on a Universal Testing Machine (Instron, 5567) with crosshead speed 50 mm/min. The degree of clay dispersion and the crystal structure of the samples were characterized at ambient temperature by means of X-ray diffraction (XRD, Bruker, D8 advance) with CuKα radiation of wavelength 1.54 Å. The acceleration voltage was 40 kV and current, 30 mA. A step size of 0.01° in the range of 1° to 30° was used. The degree of clay dispersion and distribution in the blend was confirmed by means of transmission electron microscopy (TEM, JEOL, 200CX) with an accelerating voltage of 100 kV. The nanocomposites were cryo-microtomed into specimens with an ultrathin thickness of 55 nm.

The thermal properties were determined with a differential scanning calorimeter, DSC (TA instruments, 2910). Each sample, weight 5–10 mg, was encapsulated in an aluminum pan. The experiment was carried out at a heating rate of 10°C/min from 50°C to 300°C. Crystallinity was estimated using an extrapolated value of the enthalpy corresponding to

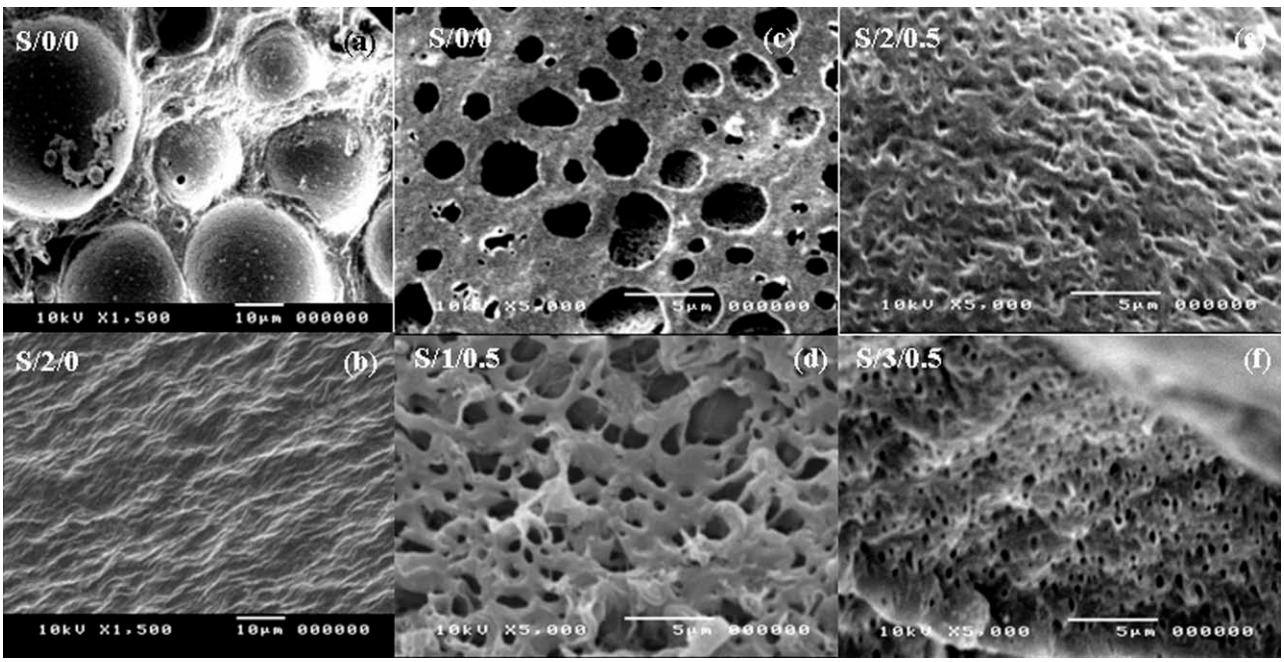

Figure 1 SEM micrographs of polymer blends (a) without and (b) with PP-MA as well as (c–f) nanocomposites after PA6 extraction while varying the amount of PP-MA.

the melting of a 100% crystalline sample: $\Delta H_{PP} = 137.9$ J/g and $\Delta H_{PA6} = 190$ J/g.[21]

Thermomechanical properties were investigated by a dynamic mechanical analyzer (NETZSCH, DMA 242C). Tested in temperature sweep mode, the dimensions of a specimen were about 55 mm × 10 mm × 2.5 mm. The strain was applied sinusoidally with a frequency of 1 Hz. The data were collected at −80°C to 150°C. The storage modulus (E'), loss modulus (E''), and damping curve (tan δ) were determined. The glass transition temperature was taken as the maximum point on the loss modulus curve in the temperature sweep tests.

Rheological properties of each composition were examined using rheometer (HAAKE, RheoStress 600) with parallel plate geometry in shear rate mode. The diameter of the plates was 20 mm and the gap was set to 0.5 mm. All measurements were carried out at 230°C in nitrogen environment. The apparent shear viscosity was measured in the range from 0.01 to 1 s^{-1}.

RESULTS AND DISCUSSION

The effect of compatibilizer on PP/PA6 blends and nanocomposites

SEM micrographs of the fractured surfaces of polymer blends without (S/0/0) and with PP-MA (S/2/0) are shown in Figure 1(a,b), respectively. The sample code used in this study indicates the weight ratio of S : PP-MA : OMMT, in which S or the weight ratio of PP : PA 6 is kept constant at 13 : 6 by weight. In Figure 1(a), PA6 domain phases are relatively large with round shape due to high-interfacial tension between polarity-dissimilar PP and PA6. When PP-MA compatibilizer was added into a polymer blend, S/2/0, it shows much more homogeneous texture than S/0/0. This may be attributed to grafted copolymer formation via reaction between the anhydride group of PP-MA and the terminal amino group of PA6 during melt mixing. The reaction was confirmed via FTIR technique.[2,20,22,23] Figure 1(c–f) shows the morphology of the etched surfaces of the nanocomposites as the PP-MA content increased. When compared with the etched surface of S/0/0, all compatibilized nanocomposites show much smaller PA6 domains, which indicate that the average PA6 domain sizes were substantially reduced owing to the presence of the compatibilizer. With an addition of one to three parts of PP-MA, the sizes of dispersed phase became rather uniform, thereby indicating strong interaction between PP and PA6 due to reactive compatibilization with PP-MA. As mentioned above, a major function of the compatibilizer is to reduce the interfacial tension and stress transfer between the components in melt state, thereby resulting in finer dispersion in the blend.

XRD and DSC techniques were used to investigate the effect of the compatibilizer on the crystallization of the polymers. Table I shows the degrees of crystallinity of PP and PA6 in nanocomposites with various PP-MA contents obtained by calculating from

TABLE I
Degree of Crystallinity and Mechanical Properties of PP/PA6 Blends and Nanocomposites

Sample code	Degree of crystallinity of PP (%)	Degree of crystallinity of PA6 (%)	Tensile modulus (GPa)	Tensile strength (MPa)	Elongation at break (%)	Flexural modulus (GPa)	Flexural strength (MPa)	Impact energy (J/m)
S/0/0	59.31	38.79	1.21 ± 0.04	33.8 ± 1.03	8.22 ± 1.20	1.93 ± 0.05	30.35 ± 0.69	9.85 ± 0.23
S/0.5/0.5	42.10	9.12	1.58 ± 0.05	37.8 ± 0.96	7.60 ± 1.57	2.36 ± 0.06	35.05 ± 0.99	8.55 ± 0.56
S/1/0.5	45.19	8.75	1.56 ± 0.03	37.4 ± 0.58	7.64 ± 0.41	2.42 ± 0.04	35.46 ± 0.62	9.89 ± 1.36
S/2/0.5	42.07	8.17	1.51 ± 0.03	36.8 ± 0.74	7.15 ± 0.61	2.66 ± 0.06	41.27 ± 0.71	8.96 ± 0.53
S/3/0.5	41.07	8.35	1.46 ± 0.04	36.3 ± 0.21	6.95 ± 0.47	2.47 ± 0.05	36.78 ± 0.50	9.99 ± 0.70
S/2/0	45.72	9.57	1.46 ± 0.03	34.0 ± 0.38	16.13 ± 0.95	2.54 ± 0.07	38.59 ± 0.77	10.27 ± 0.67
S/2/1	41.95	7.98	1.68 ± 0.03	39.9 ± 0.29	5.12 ± 0.17	2.68 ± 0.05	41.24 ± 1.11	8.06 ± 0.29
S/2/1.5	44.52	7.91	1.89 ± 0.06	34.0 ± 0.73	4.16 ± 0.15	2.77 ± 0.05	38.23 ± 1.08	7.75 ± 0.44

the enthalpy from DSC thermograms as shown in Figure 2(a). It was confirmed that the addition of PP-MA created interactions between the amide groups of the PA6 and the functional groups of the modified PP. Associated with the degree of crystallinity of PP and PA6, the measured enthalpy then decreased, which is consistent with published XRD analysis.[24] Moreover, XRD patterns (2θ in the 10–30° range) were used to determine the crystal structure of the polymers in the nanocomposites. Figure 2(b) shows the XRD patterns of nanocomposites with various compatibilizer levels. The observed peaks at 2θ = 14°, 16.8°, 18.6°, 21°, and 21.8° corresponded to the (110), (040), (130), (111), and (131) planes, respectively, of α-PP.[25] Another peak at 2θ = 21.3° corresponds to the γ-form of the PA6 component. Interestingly, the peak position of every crystal plane did not shift in the presence of PP-MA, which indicated that the α-PP and γ-PA6 crystal structure of PP and PA6 did not change.

In Table I, the incorporation of PP-MA (S/2/0) in the PP/PA6 blend (S/0/0) increased the tensile and flexural moduli, and impact energy of PP/PA6 blends by 21%, 32%, and 4%, respectively. Interestingly, the addition of only two parts of PP-MA doubled the elongation at break of the S/2/0 sample due to copolymer formation, which improved the interfacial adhesion between PP and PA6 phases[20] and increased interfacial area between PP and PA6.[5] Although PP-MA reduced the degree of crystallinity of PP and PA6 in S/2/0 by 23% and 75%, respectively, the stiffness and ductility of PP/PA6 blend (S/2/0) were enhanced due to the adhesion bond between PP and PA6 and finer domain dispersion of PA6 phase in the PP matrix, as seen in Figure 1.

As the content of PP-MA in the nanocomposites was increased from 0.5 to 3 parts (S/0.5/0.5, S/1/0.5, S/2/0.5, and S/3/0.5), their tensile moduli and tensile strength decreased by 10.8% and 4.2%, respectively. These results reveal the effects of plasticization due to the low molecular weight of PP-MA,[20] chain scission by maleic anhydride on PP-MA chain,[14] and low degree of crystallinity of PP and PA6 phases. However, the flexural modulus and flexural strength of the nanocomposites increased as the amount of PP-MA increased from 0.5 to 2 parts

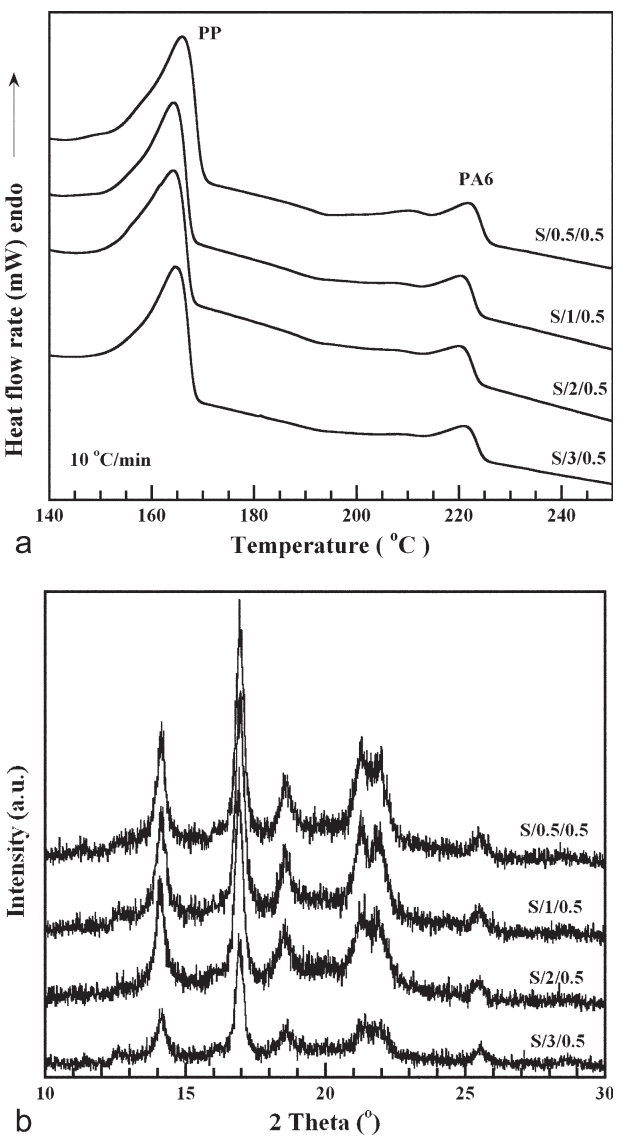

Figure 2 (a) DSC thermograms and (b) XRD patterns of nanocomposites while varying the amount of compatibilizer.

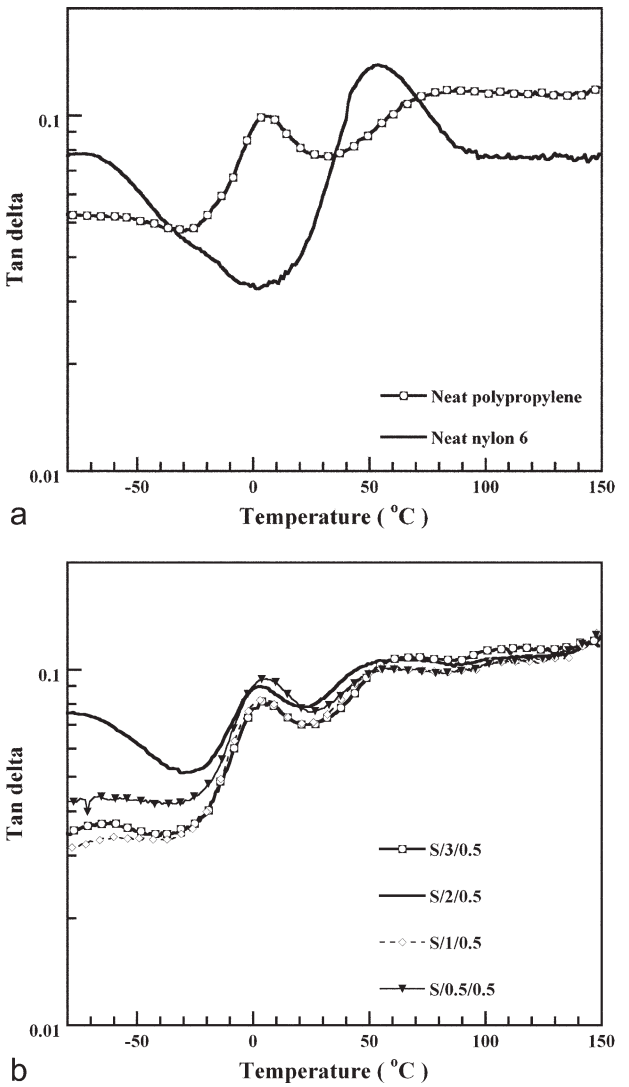

Figure 3 Tan δ of (a) neat polymers and (b) nanocomposites while varying the amount of compatibilizer.

(S/0.5/0.5, S/1/0.5, and S/2/0.5) and instead decreased when 3 parts of PP-MA was added (S/3/0.5) possibly due to an excess of PP-MA. As mentioned above, though PP-MA was used to improve interfacial adhesion between PP and PA6 phases, it can hinder the mechanical properties due to its short chain and chain scission effect.

The effect of the compatibilizer on the properties, structure mobility, and relaxation of the polymer chains of the nanocomposites were also studied by means of dynamic mechanical analysis (DMA). The values of tan δ of neat PP and neat PA6 as well as those of the nanocomposites are plotted as a function of temperature in the range of −70°C and 150°C in Figure 3(a,b). Three dynamic relaxation peaks of the nanocomposties appeared in the plot. Two relaxation peaks of PP were observed around 0°C and 85°C. The dominant relaxation peak appearing at 0°C is the glass transition of PP, which is associated with the movement of large-chain segments, whereas the weak peak appearing as a shoulder at 85°C is associated with the crystalline region of PP. The glass transition of PA6 showed up as a peak at 55°C. Maleic anhydride on PP chains (PP-MA) affected the PA6 phase more than the PP phase and, as a consequence, it resulted in a low degree of crystallinity in the PA6 phase, which was confirmed by DSC technique and can be seen in the reduction of the magnitude of PA6 glass transition peak. Meantime, the glass transition peak of PP in the nanocomposites was slightly shifted to a lower temperature as the PP-MA content increased. It is reasonable to conclude that PP-MA exerted chemical–physical influence on the crystalline properties of the PP and PA6 phases.[24]

In many practical applications, it is important to know how the apparent viscosity changes when the applied shear rate (and shear stress) has changed. The relationship between the apparent shear viscosity and shear rate for the nanocomposites with various compatibilizer contents is shown in Figure 4. The flow curves of neat PP and PA6 exhibited Newtonian behavior in the shear rate range (0.01–1 s^{-1}). However, the flow curves of the nanocomposites possessed two distinct regions, i.e., the Newtonian region and a shear-thinning region. The Newtonian region or a plateau was observed at very low shear rates, where the apparent viscosity is independent of the shear rate. In the shear-thinning region, the viscosity decreased with an increasing shear rate on the log–log plot. In short, all sets of the nanocomposite melts exhibited shear-thinning behavior (i.e., pseudoplasticity). When compared with neat PP and neat PA6, the flow curves of the nanocomposites showed much higher viscosities, especially at a low shear

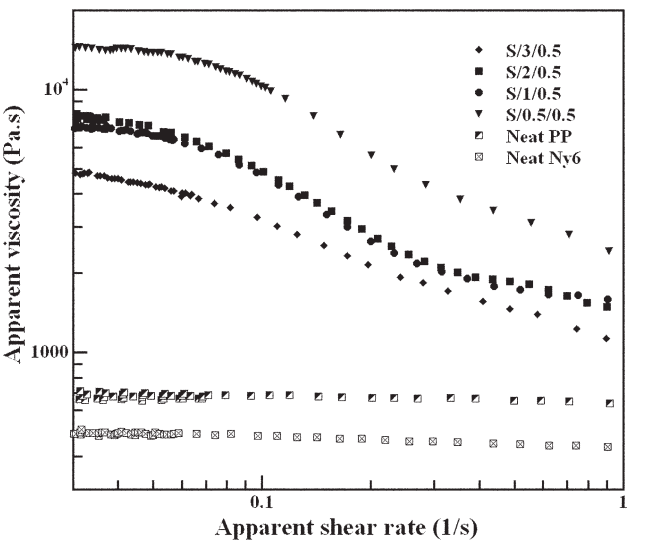

Figure 4 Apparent viscosity of nanocomposites as a function of shear rate with different compatibilizer contents.

rate, because the polar functional group in PP-MA interacted with the polar functional group of PA6, whereas the backbone of PP-MA was well mixed with PP. By the way, as the PP-MA content increased, the viscosity of the nanocomposites decreased. This could be ascribed to the low MW of PP-MA, the chain scission effect,[14] and smaller dispersed domains of PA6 in the PP matrix.

The effect of nano-reinforcing filler on the nanocomposites

Organoclay (OMMT) was added to improve the mechanical, thermal, and thermomechanical properties of the PP/PA6 blends. However, it was found out that the addition of OMMT reduced the degree of crystallinity of both PP and PA6 phases in the nanocomposites. XRD patterns of the nanocomposites containing 0–1.5 parts of OMMT (S/2/0–S/2/1.5) are shown in Figure 5(a). In this figure, the peak height decreased as the OMMT loading increased, thereby indicating that the degree of crystallinity of both PP and PA6 decreased. Evidently, the presence of clay platelets interfered with the recrystallization of both PP and PA6. Nevertheless, the XRD patterns of these nanocomposites in the range of 10–30° did not change, thereby indicating that the crystal structure of both PP and PA6 was still in the α and γ forms, respectively. In short, OMMT hindered the crystallization but did not alter the crystal form of both polypropylene and nylon 6. Table I shows the degree of crystallinity of both PP and PA6 phases in the nanocomposites estimated via the DSC technique. By adding 0.5 parts of OMMT in the polymer blend, the degree of crystallinity of the PP and PA6 phases (S/2/0.5) decreased 8.7 and 13.1%, respectively. This phenomenon was consistent with the XRD results.

In Figure 5(b), the XRD technique was used to identify how the OMMT was dispersed in the polymer matrix. The XRD patterns of pure OMMT and nanocomposites with 0.5–1.5 parts of OMMT content are shown in the range of 1–10°. The diffraction peak of pure organoclay was located at $2\theta = 4.43°$. Based on Bragg's equation, $2d \sin\theta = n\lambda$, the interlayer spacing of OMMT became equal to 1.99 nm. For both S/2/0.5 and S/2/1, small broad peaks were observed at $2\theta = 3.92°$ and 3.97°, which corresponded to *d*-spacing of 2.25 nm and 2.22 nm, respectively. The XRD pattern of S/2/1.5 nanocomposite shows a broad shoulder around $2\theta = 3°$ and well-defined peak at $2\theta = 3.98°$ ($\cong$2.22 nm), thereby indicating that the layered silicates were in order. The XRD patterns of both S/2/0.5 and S/2/1 exhibited a broad profile, which indicates structural disorder and inhomogeneity in the interlayer composition of the specimens. The broad peak indicated the occurrence of partial exfoliation.[26] Polymer chains might intercalate between layered silicates of the OMMT and resulted in larger interlayer spacing between the platelets. The above XRD results can also be verified by TEM micrographs. Figure 6 shows the TEM micrograph of S/2/0.5 nanocomposite, which had the lowest clay content. The nylon 6 domains in SEM image in Figure 1(e) and the domains in the first TEM image show similar sizes. When the domains were magnified as seen in the second image, it reveals that most of the layered silicates were found at the interface between PP and PA6. The second and third TEM images show the intercalated structure with varying interlayer spacing of clay platelets. Therefore, the low intensity of

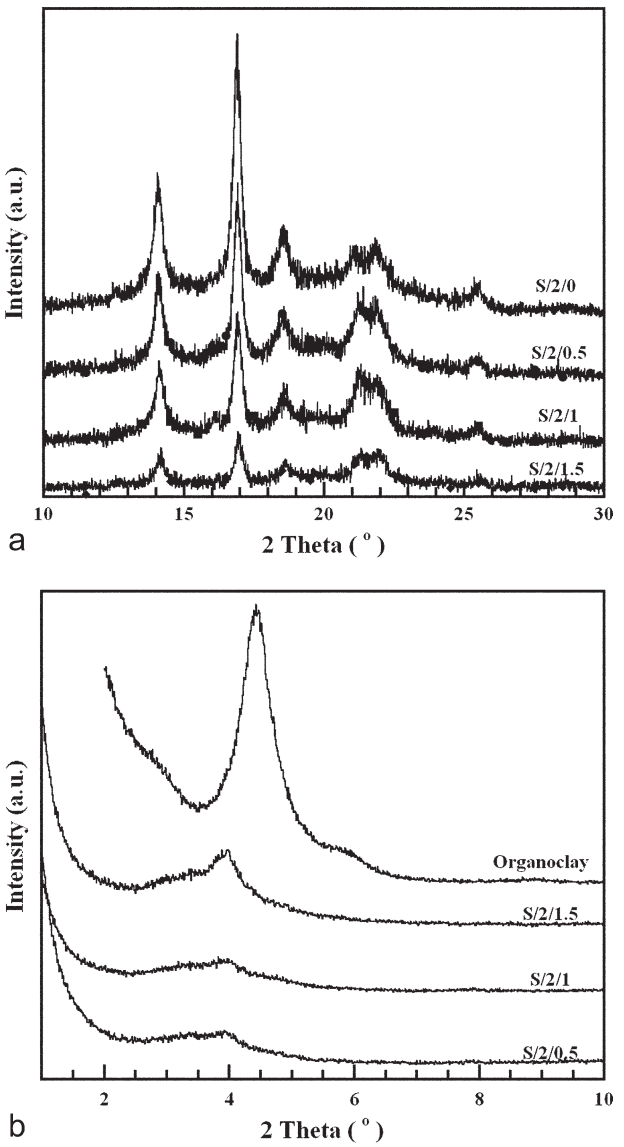

Figure 5 XRD patterns of nanocomposites with different filler contents (a) crystal structure of polymers and (b) degree of clay dispersion.

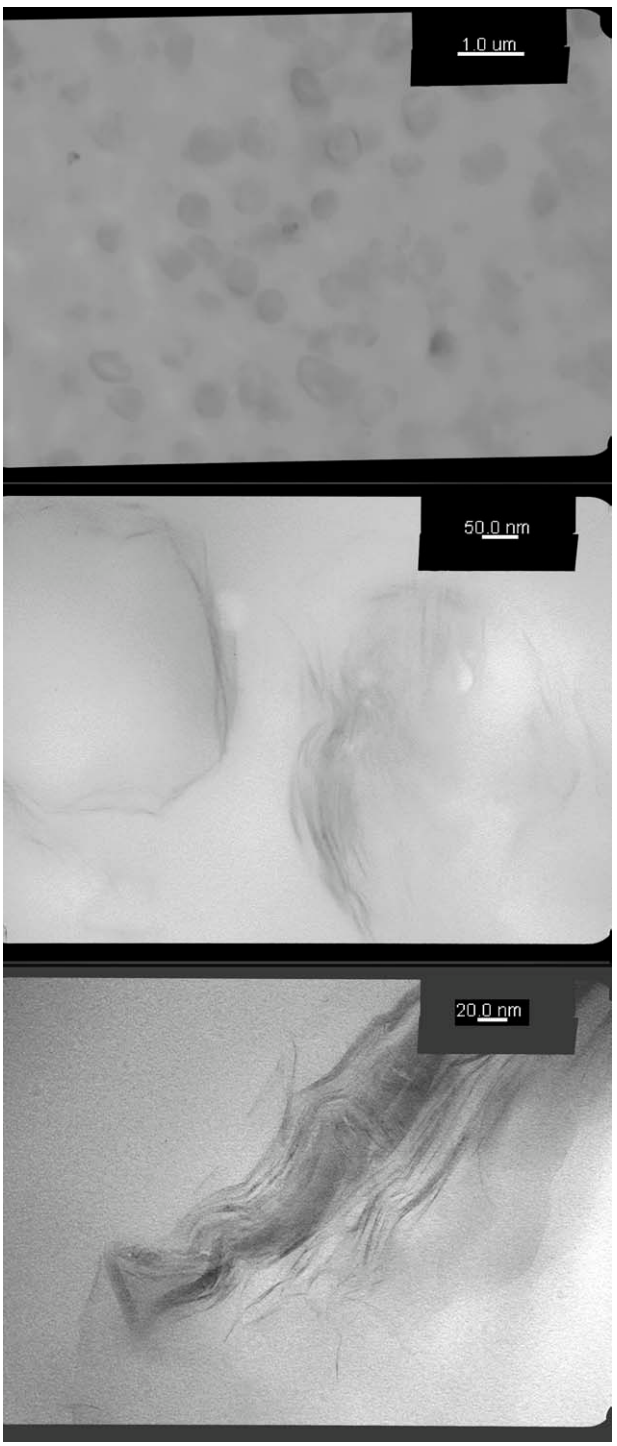

Figure 6 TEM micrographs of PP/PA6/clay nanocomposites with 0.5 parts of clay (S/2/0.5).

XRD peak of the sample is observed, which is consistent with these TEM images.

The effects of the organoclay (OMMT) on the mechanical properties of the nanocomposites such as tensile, flexural, and impact properties are given in Table I. The addition of OMMT led to substantial improvement in the stiffness of the PP/PA6 blends. OMMT addition also enhanced the tensile modulus of the nanocomposites. For example, adding 1.5 parts of OMMT (S/2/1.5) increased the tensile modulus by 29.5% compared with the polymer blend (S/2/0). The increase in the tensile modulus indicates a decrease in the molecular mobility of polymer chains under stress. Interaction between polymer chains and OMMT reflected strong polymer/filler interactions and good molecular mixing.[27] On the other hand, addition of the organoclay reduced the elongation at break. As confirmed by both XRD and TEM, the layered silicates remained agglomerated and resided at the PP/PA6 interface. As a consequence, increasing the OMMT made the interfacial area between PP and PA6 more brittle, and the elongation at break decreased. Table I also lists the impact test values of the nanocomposites, which correspond to the capacity of energy absorption by the material before breaking, i.e., its toughness. An increment of the OMMT decreased the impact energy of the nanocomposites. It can be considered that the addition of OMMT diminished the ductility caused by the inhomogeneous structure of the nanocomposites.

The flexural modulus and flexural strength at different OMMT contents are also listed in Table I. By adding 0.5–1.5 parts of OMMT, the flexural modulus increased in the same trend as the tensile modulus. The observed behavior can be attributed to the effect of the increment on the increased surface area between OMMT and polymer matrix. For example, adding 1.5 parts of OMMT in the S/2/1.5 nanocomposite increased the flexural modulus by 9% compared with the S/2/0 polymer blend. Although the flexural modulus of the nanocomposites was continuously improved, the flexural strength became lower as the OMMT content increased because of the increased interaction with OMMT, e.g., by bridging, hampered the uniform distribution of the OMMT filler, thereby resulting in the lower flexural strength of the nanocomposites.

Figure 7(a,b) shows the storage modulus (E' modulus) and tan δ of the nanocomposites, respectively, as a function of temperature. By adding 0.5, 1, and 1.5 parts of OMMT, the storage modulus increased by 12.7%, 20.5%, and 21.6%, respectively, compared with that of neat PP. In the room temperature range, S/2/1.5 shows the least deformation caused by an applied load because of its highest storage modulus. This is consistent with the result of the flexural modulus, as discussed earlier. In the rubbery transition region, all nanocomposites showed little difference in the storage modulus whereas PP showed the lowest storage modulus. This indicates that these nanocomposites had similar thermal stability characteristics.

An increase in the OMMT loading enhanced the storage modulus of the nanocomposites due to a

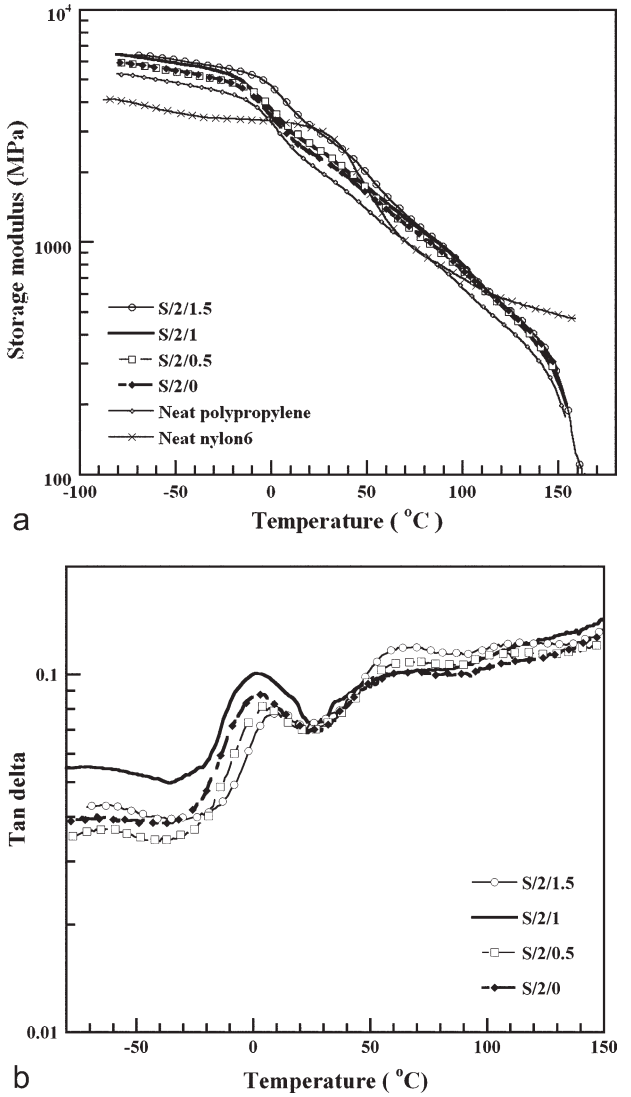

Figure 7 DMA measurements of nanocomposites at different organoclay contents: (a) storage modulus (b) tan δ.

corresponding decrease in molecular mobility of polymer chains as a consequence of the interaction between the chains and OMMT. Because the OMMT filler is known to possess high stiffness, the mobility of the matrix can severely be restricted by this filler upon adhesion to the filler surface. This also led to a decrement in the glass transition temperature of the nanocomposites and a tendency to interfere with crystallization. The effect of the OMMT content on the glass transition temperature is shown in Figure 7(b) in terms of DMA measurements. Three relaxation peaks were observed: at 0°C, a weak peak appearing as a shoulder at about 50–70°C, and 110°C. They corresponded to the glass transition temperature of PP, another relaxation of PP, and the glass transition of the dispersed phase of PA6, respectively. Figure 7(b) confirms the effect of OMMT on the elevation of glass transition temperature of the resulting nanocomposites. The glass transition temperature of the neat PP is 5.3°C. By making the polymer blend, S/2/0, the glass transition temperature of PP phase was shifted to 2°C. By adding 1.5 parts of OMMT, the relaxation peak of PP in the nanocomposites took place at 10°C, which is much higher than that of the polymer blend without OMMT. The layered silicates restricted the segmental motion of polymer molecules. As a consequence, the glass transition temperature rose.

Many industrial processes are affected by the influence of the filler on the flow properties. The flow properties of materials can often be adjusted by varying the filler loading. In this study, 0.5–1.5 parts of OMMT loading are added to the polymer blends, as shown in Figure 8. The apparent shear viscosity of the nanocomposites showed significant enhancement in their zero-shear viscosity because interactions with the layered silicates became stronger at higher OMMT contents, where the distance between the layers became shorter. In fact all sets of polymer nanocomposite melts exhibited shear-thinning behavior. The high zero-shear viscosity of the nanocomposites indicates that, at low-shear rates, the nanostructure of these materials displays strong interaction between the dispersed clay platelets and polymer chains. As observed in many filled systems, the steady shear viscosity of the layered silicate nanocomposites depended on the clay content and interactions between clay particles.[28]

CONCLUSIONS

As expected, this study suggests that both the compatibilizer and organoclay wield significant effects on the mechanical, thermal, thermomechanical, and rheological properties as well as the microstructure

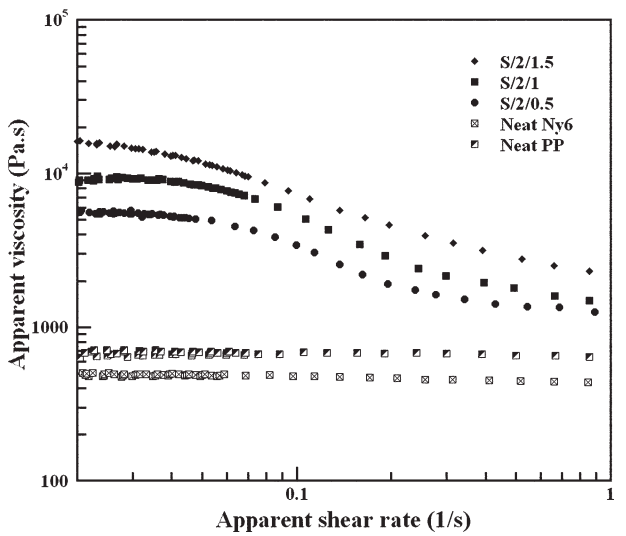

Figure 8 Apparent viscosity of nanocomposites as a function of shear rate at different organoclay loading.

of the nanocomposites. The compatibilizer hindered crystallization of both the PP and PA6 phases but did not change their crystal structures. Therefore, by improving the interfacial adhesion between the polymer phases, the solid-state mechanical properties of the nanocomposite can significantly be improved. The glass transition temperature of the nanocomposites decreased as the PP-MA compatibilizer increased due to the low molecular weight of PP-MA and chain scission by maleic anhydride.

Incorporation of the organoclay improved the tensile modulus by 30%. The glass transition temperature increased as the OMMT loading increased because of the contribution of the strong interaction between the OMMT and the polymer matrix and the restriction by OMMT of the mobility of polymer matrix.

The authors thank the Department of Physics, Mahidol University, for the use of XRD and the Center for Advanced Materials Analysis, Tokyo Institute of Technology, for TEM images.

References

1. Mehdi, A.; Richard, K.; Mohammad, H.; Hosein, N.; Bhupender, S. Polymer 2002, 43, 1331.
2. Roeder, J.; Oliveira, R.; Goncalves, M.; Soldi, V.; Pires, A. Polym Test 2002, 21, 815.
3. Verdier, C.; Vinagre, H. T. M.; Piau, M.; Joseph, D. D. Polymer 2000, 41, 6683.
4. Chow, W. S.; Abu Bakar, A.; Mohd Ishak, Z. A.; Karger-Kocsis, J.; Ishiaku, U. S. Eur Polym J 2005, 41, 687.
5. Gonzalez, I.; Eguiazabal, J.; Nazabal, J. Compos Sci Technol 2006, 66, 1833.
6. Xiong, J. W.; Zheng, Z.; Jiang, H. M.; Ye, S. F.; Wang, X. L. Compos A 2007, 38, 132.
7. Tedesco, A.; Barbosa, R.; Nachtigall, S.; Mauler, R. Polym Test 2002, 21, 11.
8. Tseng, F.; Lin, J.; Tseng, C.; Chang, F. Polymer 2001, 42, 713.
9. Kusmono, Z. A.; Chow, W. S.; Takeichi, T.; Rochmadi. Eur Polym J 2008, 44, 1023.
10. Osman, G. E.; Nihan, N. Polym Bull 2003, 49, 465.
11. Fornes, T.; Paul, D. Polymer 2003, 44, 3945.
12. Arunvisut, S.; Phummanee, S.; Somwangthanaroj, A. J Appl Polym Sci 2007, 106, 2210.
13. Osman, A.; Jorg, R.; Suter, U. Polymer 2005, 46, 1653.
14. Solomon, M. J.; Almusallam, A. S.; Seefeldt, K. F.; Somwangthanaroj, A.; Varadan, P. Macromolecules 2001, 34, 1864.
15. Somwangthanaroj, A.; Lee, E. C.; Solomon, M. J. Macromolecules 2003, 36, 2333.
16. Zilg, C.; Thomann, R.; Mulhaupt, R.; Finter, J. Adv Mater 1999, 11, 49.
17. Fu, X.; Qutubuddin, S. Polymer 2001, 42, 807.
18. Ruowen, Z.; Yuan, H.; Shaofeng, W.; Lei, S. Polym Degrad Stab 2004, 83, 423.
19. Kim, H. B.; Choi, J. S.; Lee, C. H.; Lim, S. T.; Jhon, M. S.; Choi, H. J. Eur Polym J 2005, 41, 679.
20. Chow, S.; Mohd, I.; Karger, J.; Apostolovc, A.; Ishiakud, S. Polymer 2003, 44, 7427.
21. Braumpdrup, J.; Immergut, E. H. Polymer Handbook; Wiley: New York, 1989.
22. Sathe, S. N.; Devi, S.; Rao, G. S. S.; Rao, K. V. J Appl Polym Sci 1996, 61, 97.
23. Sathe, S. N.; Rao, G. S. S.; Rao, K. V.; Devi, S. Polym Eng Sci 1996, 36, 2443.
24. Campoy, I.; Arribas, J. M.; Zaporta, M. A. M.; Marco, C.; Gomez, M. A.; Fator, J. G. Eur Polym J 1995, 31, 475.
25. Feng, M.; Gong, F.; Zhao, C.; Chen, G.; Zhang, S.; Yang, M.; Han, C. C. J Polym Sci Part B: Polym Phys 2004, 42, 3428.
26. Alexandre, M.; Dubois, P. Mater Sci Eng R Rep 2000, 28, 1.
27. Saujanya, C.; Radhakrishnan, S. Polymer 2001, 42, 6723.
28. Hyun, Y. H.; Lim, S. T.; Choi, H. J.; Jhon, M. S. Macromolecules 2001, 34, 8084.